Gas-Phase Surface Engineering of Polystyrene beads used to challenge Automated Particles Inspection Systems

*Vickie Labonté, Antoine Marion, Nick Virgilio, Jason R. Tavares**

CREPEC, Department of Chemical Engineering, Polytechnique Montreal, P.O. Box 6079, stat. Centre-Ville, Montréal (Quebec), H3C 3A7

KEYWORDS: Chemical Vapor Deposition, UV Treatment, Syngas, Ozone, Polymer beads, Coating, Wettability, Dispersion Stability, Thin Film

ABSTRACT: Container challenge sets, used in the qualification and validation of automated visible particle inspection systems in the parenteral drug industry, are prepared by seeding a single standardized polystyrene-divinylbenzene (PS-DVB) bead inside the commercial product to mimic foreign particulates. Due to its low surface energy and wettability, the bead adheres to container walls, hindering its detection by the motion based inspection system. The aim of this research is to modify the surface properties of the bead in such a way that it repulses the inner walls and stays in suspension inside the liquid product. The surface treatment consists of a photo-induced chemical vapor deposition (PICVD) process using syngas and UVC light. Following

treatment, newly grafted C-OH, C-O-C, C=O and COOH functional groups on the bead's surface are observed by XPS and FTIR spectroscopy, leading to an increase in the surface energy from 31 ± 1 to 65 ± 2 mJ/m^2, and a corresponding zeta potential decrease from -38 mV to -61 mV. Finally, treated 100 μm, 200 μm and 500 μm PS-DVB beads suspended in water exhibit higher dispersion stability over time than untreated beads. These results show the potential of syngas PICVD to provide an effective solution to the stability issue of containers challenge sets for the validation of automated particle inspection systems, enabling significant savings of time and money to the parenteral drug industry.

INTRODUCTION

Intravenous injection is the second most widely used means for delivering a drug to a patient, after oral ingestion. Indeed, the global market of prefilled syringes is likely to generate receipts of $7 billion by 2018, as sales have increased at a compounded annual growth rate of 14% since 2012.[1] This represents around 190 million liters of parenteral drugs per year injected in patients, only in the United States.[2] On the other hand, major incidents of venous occlusion, organ damage, pulmonary embolism and granulomatosis in patients following injection of a parenteral drug containing foreign particulates have been reported in the past forty years.[3-6] To prevent future clinical incidents and ensure product safety, regulatory agencies require parenteral drugs to be "essentially free" of solid contaminants before reaching the consumers.[2] To meet this requirement, manufacturers make extensive use of automated particle detection systems, since it is quicker and more consistent than human inspectors, who are subjective and experience fatigue.[7-10] The inspection principle relies on the tracking of foreign particulates' motion inside the liquid media, observed after syringe swirling.[7] In the past years, there has been an increase in

the number of product recalls due to particulate contamination,[11-13] which has led to rising regulatory activity around the qualification and validation of automated particle detection systems.[10] The validation of particle detection systems requires the use of standard challenge sets.[7] These are prepared by seeding a single particle to mimic contamination inside a sterilized syringe filled with either water for injection (WFI) or a mimic solution of the drug product. Each control syringe is then swirled and inspected by a camera that detects the movement of the seeded bead. The system is then supposed to sort and extract the control syringe from the production line. Adequate challenge sets must be stable and provide reproducible results in the long-term, i.e. 3 to 5 years.[8] NIST spheres, usually made of polystyrene, stainless steel, glass or various resins, are stable, robust, and suitable for extensive use in control syringes. However, a lack of bead wettability and low surface energy often lead to its irreversible sticking to the inner walls of prefilled syringes, thereby hindering particle motion and rendering micro-bead detection impossible.[8, 14] This is a major concern that leads to the frequent replacement of control syringe sets and generates significant costs of time and money for what is intended to be a simple day to day validation step. Although use of surfactants can maintain the standard sphere in suspension and prevent its adhesion, surfactants also tend to stabilize air bubbles under vortex swirling. The particle detection system does not make a distinction between air bubbles and quality control beads, which leads to the emergence of false-positive results.[7, 15]

The goal of this research is to solve the "stickiness" issue by developing a surface treatment that would prevent wall adhesion of polystyrene-divinylbenzene (PS-DVB) NIST beads inside WFI syringe challenge sets by increasing their surface charge, and thus their repulsion with syringe walls. Over time, many surface modification techniques have been explored to increase polystyrene's wettability and surface energy for a wide variety of

applications. The oldest processes are wet chemical techniques.[16-20] Polystyrene functionalization employing atomic oxygen treatments[17, 21] is a well-documented example of such wet chemistry approaches. However, the complex downstream treatment of costly and sometimes hazardous solvents hinders the application of wet chemistry approaches on a larger scale. Chemical vapor deposition (CVD) represents a viable alternative as a dry, solvent-free process. Traditional CVD uses heat as the energy source required for functionalization, although CVD variants using plasma or UV light are preferred to functionalize substrates sensitive to heat[22] such as polystyrene. Radio frequency[23] and microwave[24-25] plasma CVD efficiently functionalize polystyrene both at low pressure[3] or atmospheric pressure,[26] using either oxygen (O_2),[25, 27] argon (Ar),[23, 25, 28-29] air [30] or helium/nitrogen mixtures (He/N_2)[31] as gas precursors. In order to maximize functional groups retention, keep a better control on the process and save costs, one would prefer to replace plasma CVD by luminous CVD, since the latter employs a lower energy source such as light. Indeed, luminous CVD allows for the targeting of specific reaction pathways, since only select compounds and bonds will react as a function of the wavelength used. ArF excimer laser irradiation with oxygen (O_2),[32-33] gamma irradiation,[19] UV radiation combined with ozone (O_3),[18, 26, 34-42] air [33] or ammonia (NH_3)[41] and vacuum-UV (VUV, 172 nm) with air,[43] are all alternative functionalization techniques that have been tested on polystyrene with success. Among these, treatments combining UV and O_3 (UV-ozone) is of interest because of design simplicity, operation close to ambient conditions, relative low cost, controllability and generally harmless waste products, since ozone is a thermodynamically unstable precursor[44] quickly reconverted to oxygen. However, the major drawback of UV-ozone treatments is that most of the functionalization does not last over time.[35, 41-42] Functional group retention might be

improved by replacing ozone with another chemical precursor that would be able to polymerize when exposed to UV-light.

Syngas is a mixture of carbon monoxide (CO) and hydrogen (H_2) that can be used to build carbon chains by polymerization according to the Fischer-Tropsch pathway.[45] Given that polystyrene's vinyl groups are known to produce radicals upon exposure to UVC (200-280 nm) light through the scission of π-bonds[46], the question remains if a reaction mechanism similar to free radical polymerization could occur when polystyrene beads are exposed to both syngas and low energy UVC radiation. Surface grafting of sufficiently long polymer chains containing oxygen groups could stabilize a suspension of PS-DVB beads due to both electrostatic and steric effects.[47] We thus expect treated beads to remain stable in suspension without additives, thus enabling automated detection after container swirling over extended periods. Radical polymerization of syngas initiated by UVC radiation has already been tested on copper,[48] polypropylene and polyethylene terephthalate[49], nanocrystalline cellulose[50], superparamagnetic iron oxide nanoparticles[51] and metal oxide nanoparticles[52] substrates with success.

In this study, we propose surface grafting of hydrophilic groups on NIST PS-DVB beads through a Photo Initiated Chemical Vapor Deposition (PICVD) technique using syngas as the precursor, and operating at near-ambient conditions. For this research, PS-DVB particles seeded in challenge syringes filled with WFI are being used as a case study since they are a recognized standard in the pharmaceutical industry. The differences in surface chemical composition, surface properties and suspension stability are compared before and after treatment. The syngas PICVD treatment is also compared with UV-ozone surface oxidation.

EXPERIMENTAL SECTION

Materials. Polystyrene 615 APR granules were purchased from the Dow Chemical Co. PS-DVB standard 5 !m, black-dyed Chromosphere-T 100 !m, 200 !m and 500 !m were purchased from ThermoScientific (DC05, BK100T, BK200T and BK500T, 1 gram per bottle). Argon HPT, Hydrogen UHP T-30 and Pure T-44 Carbon Monoxide were purchased from Air Liquide Canada. WFI was simulated by using water from Polytechnique Montreal s supply, purified using a Synergy 185 water purificator (Millipore) and filtered using Whatman grade 4 filter papers (mesh size 20-25 !m). Isopropyl alcohol (70% USP) was obtained from GreenField Ethanol Inc., while hydrogen peroxide (50%) and n-hexadecane were obtained from Fisher Chemicals (New-Jersey). Silicon fluid 10 cst was obtained from Wacker (Germany) and white mineral oil Puretol 7S was obtained from Petro Canada (Ontario). The TS-40 Turn-Key Ozone Generator was leased from Ozone Solutions (IA) to produce O_3 from ambient air by corona discharge. The ozone generator was connected to the reactor inlet with a " inch OD teflon tube (McMaster). Polypropylene syringes were supplied by Liebel-Flarsheim Canada Inc. Pharmaceuticals (Montreal). The cleaning product used to wash the interior of syringes was Contrad 70 cat no 1003 from Decon Laboratories Inc.

Preparation of Polystyrene films and PS-DVB beads. Since some of the surface characterization techniques employed in this work function more efficiently with flat substrates, polystyrene films were used as a substitution substrate to PS-DVB beads for a few characterisation tests such as contact angle measurement, FTIR spectroscopy, XPS and AFM. Polystyrene 615 APR granules were cleaned inside an ultra-sonification bath (FS110H Fisher Scientific) with 70% v/v iso-propanol in water for fifteen minutes. Granules were then soaked in DI water for 30 min at ambient temperature (~22¡C) and allowed to dry overnight in a dessicator

(Bel-Art Products) under vacuum. Cleaned and dried polystyrene granules were sandwiched between two polyamide films and heated to 400¡F for 5 min before being compressed in a Carver micropress at 400¡F and 1.5 atm for another 5 min in order to form films (thickness 162 ± 4 μm). These films were then cut into 2x1 cm pieces and inserted directly into the reactor for treatment. The PS-DVB beads from ThermoScientific were taken directly from the supply bottle and deposited on a glass support previously cleaned with 70% iso-propanol and dried using Kimwipe paper.

Surface Functionalization in the PICVD reactor. The reaction chamber consists of two 45 x 2.5 cm quartz tubes connected end-to-end and illuminated by two 30 W UVC mercury lamps (Cole-Parmer VL-230-G) both emitting at 253.7 nm with an average irradiance of 0.38 ± 0.05 mW/cm^2 at a distance of 2 cm. The irradiance was measured with an ILT 1700 Research Radiometer (International Light Technologies) coupled with a SED240 detector. Syngas or ozone is allowed to flow inside the reaction chamber where it can react with the polystyrene substrate (Figure 1).

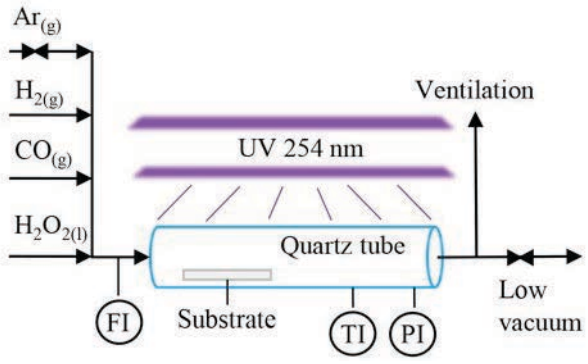

Figure 1: Scheme of the photo-initiated chemical vapor deposition reactor operating with syngas

The flow rate of syngas does not exceed 500 mL/min to ensure a sufficiently high residence time inside the reactor; individual flow rates were adjusted using a mass flow controller (Brooks Instrument, model 5878). In the case of surface functionalization with ozone, the inlet gas is

composed of O_2 with a low percentage of ozone (5-7% w/w). In all cases, argon is used to purge the system before and after an experiment. Hydrogen peroxide 50% v/v is injected inside the reactor using a syringe pump (Cole-Parmer¤, model 200) at a rate of 1 mL/h; it is used as a photo-initiator for the polymerization reaction with syngas. Treatment time is 1 hour at 33 ± 1 ¡C. The reactor pressure, sample positioning inside the reactor, flow rate of H_2O_2 and H_2/CO mass ratio of syngas were tuned as part of the experimental plan.

Surface Characterization of PS films

Atomic Force Microscopy (AFM). Topographic characterization was done in tapping mode using an ACTA pyramidal tip and an Si cantilever (Applied Nano Inc.) with a Multi-Mode 3 AFM device (Bruker AS-130 J). The nominal spring constant of the cantilever is 37 N/m and its response frequency is 300 kHz. The tip's radius of curvature is 6 nm. The images were taken at a scan rate of 0.8-1 Hz, a resolution of 512 x 512 pixels and a scan size of 5 x 5 !m. Image analysis was conducted with the Nanoscope Analysis software.

Contact angle measurements (CAMs). Goniometry tests have been performed with a TBU 90E contact angle system (DataPhysics) using the SCA20 software. At first, the sessile drop technique was used to observe the evolution of the water contact angle measurements over time on four different syngas-treated samples. These results were compared with the ones obtained for polystyrene treated with UV-ozone. To further confirm the results obtained with water contact angle measurements, the sessile drop technique was also used to perform silicone and mineral oils and contact angles with the treated surface submerged in DI water. To verify that the density difference between oil and water would not affect the contact angle measurements, the drops were first dispensed both under and above untreated surfaces using an inverted and straight needle, respectively. Finally, in order to perform accurate surface energy

estimations, dynamic contact angle measurements from both polar and apolar media are necessary. Deionized water ($\#_w^d$ = 21.8 mN/m; $\#_w^p$ = 51 mN/m)[53] and n-hexadecane ($\#_h^d$ = 27.47 mN/m; $\#_h^p$ = 0 mN/m)[54] were selected as the polar and apolar liquids, respectively. Advancing (θ_{adv}) and receding (θ_{rec}) contact angles were recorded using the volume variation method with a drop volume of 2 ± 0.01 !L and a dispense rate of 0.15 !L/s. These measurements were repeated seven times at different regions of the substrate surface, and were repeated on three different samples to assess reproducibility. Substrate surface energy calculations were performed subsequently following the Owens and Wendt method, wherein the surface energy of polystyrene (γ_{PS}) is distributed into a dispersive (γ_{PS}^d) and a polar (γ_{PS}^p) component:[55]

$$\gamma_{PS} = \gamma_{PS}^d + \gamma_{PS}^p \qquad (1.1)$$

$$(\gamma_{PS}^d \gamma_w^d)^{0.5} + (\gamma_{PS}^p \gamma_w^p)^{0.5} = 0.5\left(\gamma_w^d + \gamma_w^p\right)\left(1 + \cos\theta_{adv}^w\right) \qquad (1.2)$$

$$(\gamma_{PS}^d \gamma_h^d)^{0.5} + (\gamma_{PS}^p \gamma_h^p)^{0.5} = 0.5\left(\gamma_h^d + \gamma_h^p\right)\left(1 + \cos\theta_{adv}^h\right) \qquad (1.3)$$

ATR-FTIR spectroscopy. Fourier-Transform Infra-Red (FTIR) spectra were acquired in Attenuated Total Reflectance (ATR) mode with a Spectrum 65 FT-IR spectrometer and Spectrum software from PerkinElmer. 32 scans per sample were collected within the 600-4000 cm^{-1} spectral range, with a resolution of 4 cm^{-1}. The infrared light incident angle on the Zn/Se crystal is 30¡; the maximum penetration depth inside the sample surface ranges between 1 and 6.5 !m for polystyrene.

X-Ray Photoelectron Spectroscopy (XPS). Further functional characterization of the surface was performed with the ESCLAB 3 MKII X-Ray Photo-Electron Spectroscopy (XPS) instrument. A Mg source at 216 W, 12 kV and 18 mA was used. The XPS chamber was kept at a $5x10^{-9}$ torr maximum pressure. The analyzed surface area was 2 mm x 3 mm and the analyzed

depth was 5-10 nm. Background noise substraction was performed according to the Shirley method.

Zeta Potential Calculation on PS-DVB standard 5 !m beads. Since PS-DVB beads used in the industry are too large to perform reliable zeta potential calculations (sedimentation effect), smaller 5 !m PS-DVB beads were used for this particular characterization technique. These were suspended in water containing 10 mM NaCl prior to analysis. The zeta potential ($) of the suspension was then analyzed with a ZetaSizer Nano ZS (Malvern Instruments) by measuring the electrophoretic mobility (m) of the beads in suspension and applying the equation following the Smoluchowski model[56]:

$$\zeta = \frac{m\eta}{\varepsilon} \qquad (2)$$

where η is viscosity and ε is permittivity.

Accelerated Ageing Dispersion Stability Testing. It is assumed that the chemical degradation of the treated beads over time is a reaction of zero or first order, since it is the case for a wide range of polymers.[57] The Arrhenius equation is therefore applicable:

$$AAT = Q^{[(T_{AA} - T_{RS})/10]} \cdot RAT \qquad (3)$$

where AAT = Accelerated Ageing Time

T_{AA} = Accelerated Ageing Temperature (%60¡C, to prevent non-linear changes in the polymer)

T_{RS} = Real Storage Temperature (22¡C)

RAT = Real Ageing Time at T_{RS}

Q = Ageing coefficient

For this study, an ageing coefficient of 2 has been selected, since it is a commonly used and conservative value for medical polymers.[58] It corresponds to the doubling of the degradation

rate following an increment of 10¡C in the storage temperature. To verify at least 2 years of suspension stability of the treated beads according to the Arrhenius equation, the seeded syringes have been stored at 58¡C for a testing period of 2 months.[58] For the ageing study, a total of 192 polypropylene syringes were filled with WFI: 64 were seeded with a single syngas-treated 100 !m PS-DVB bead, 64 with a 200 !m treated bead, and 64 more with a 500 !m treated bead. Half of the syringes were stored at 58¡C. The other half were stored at ambient temperature (22¡C) for comparison and further confirmation of the ageing test results. Each sample was examined once per month to see if the treated bead either stays in suspension, peels off the inner walls following a swirling step, or irreversibly stick to the inner walls of the syringe (despite swirling). For the suspension stability acceptance criteria to be met, the treated beads must at least peel off the inner walls after 2 seconds of syringe swirling at a speed of 3200 rpm. This criteria was established to mimic as accurately as possible the behavior of an automated particle detection system typically used in industry. The samples were swirled using a VWR 945301 analog vortex mixer. The interaction of the treated beads with the inner walls of the syringe before and after swirling is assessed visually.

RESULTS AND DISCUSSION

Syngas Treatment. The PICVD reaction with syngas has been tested under different sets of parameters. An optimal set of parameters was identified following a detailed design of experiment, with the H_2/CO ratio varying from 1/12 to 1, the pressure varying from 86 kPa to atmospheric (101 kPa), the sample position varying from 2.5 to 30 cm from the gas inlet and the H_2O_2 flow rate varying from 0 to 1 mL/h. After each polystyrene surface treatment, functionalization efficacy was evaluated using the sessile drop technique with DI water as the drop liquid. The native water contact angle on polystyrene lies around 95¡. At an H_2/CO ratio of

1/10, with an operating pressure of 86 kPa, coupled with a 1 mL/h H_2O_2 injection and a sample position of 10 cm, the contact angle drops to 20¡. This set of parameters was therefore retained as the optimum for polystyrene hydrophilization. The critical parameters were the position of the substrate inside the reactor, the reactor pressure and the H_2/CO mass flow ratio, consistent with the work of Dion et al.[48] The same pressure, sample position and H_2O_2 feed were used during UV-ozone treatments. The details and results of the entire experimental plan are provided as supporting information (S-1).

Atomic Force Microscopy (AFM). Topography analysis was conducted on polystyrene films both before and after treatment through atomic force microscopy (Figure 2). A scan size of 5 x 5 !m and a height scale of ± 30 nm were taken for all AFM pictures. The morphology for surfaces treated with syngas is significantly different from the untreated or UV-ozone treated surfaces. Indeed, narrow islands of 35-50 nm in height and of 70 nm in average diameter, as highlighted with green circles, are evenly distributed on the surface and form a dense pattern. Further, the island-like deposition observed by AFM is consistent with previous electron-microscopy findings on PICVD treated copper substrates.[48] Save for a few punctual observations, no significant roughness difference is observed between untreated surfaces and UV-ozone treated surfaces. On the other side, the randomly dispersed larger grains identified with yellow arrows in Figure 2 are similar to features observed in previous studies on polystyrene treated with UV and ozone,[34, 59-60] which are associated with loosely bonded fragments inherent to the oxidation effect of ozone. [34-36, 59, 61] Holes highlighted with blues circles may correspond to partial surface etching of polystyrene, known to occur under a UV-ozone treatment.[60]

a)

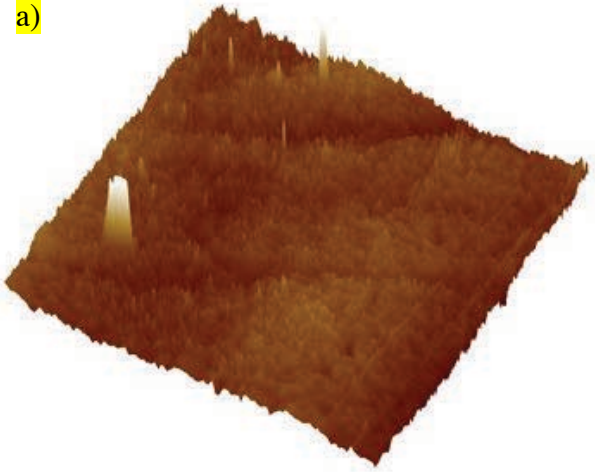

b)

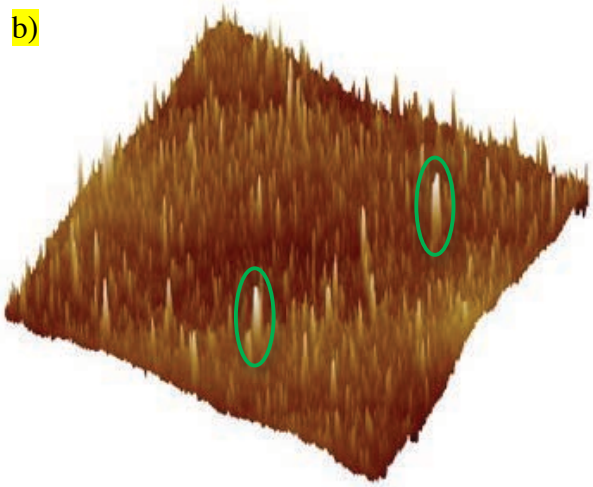

c)

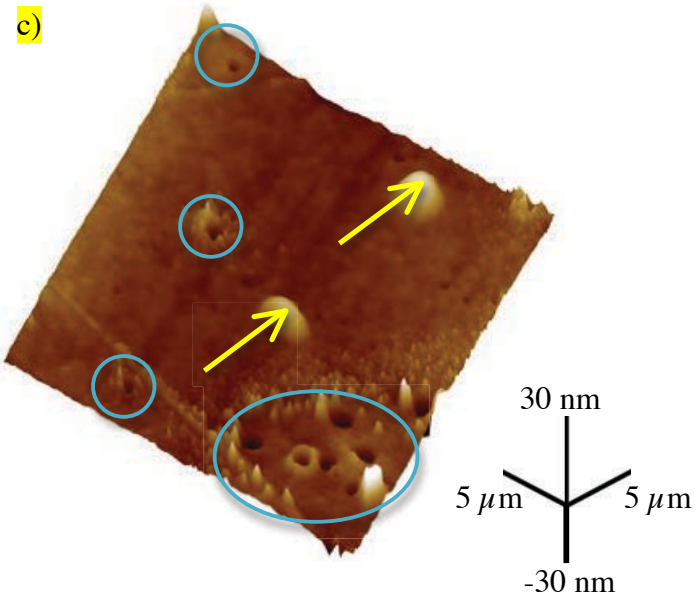

Figure 2. AFM images of PS a) untreated, b) treated with syngas and c) treated with ozone. Green circles highlight typical island features emerging from syngas treatment. Blue circles highlight spots on the surface where etching might have occurred. Yellow arrows highlights loosely bonded fragments inherent to the oxidation effect of ozone.

Water Contact Angle Measurements. Figure 3 shows a sessile drop water contact angle on polystyrene before and after treatment, while average advancing and receding contact angle measurements, total surface energy and surface energy components before and after treatment are reported in Table 1. For both syngas and ozone treatment, dynamic contact angles decrease below 30° after treatment, which correspond to highly hydrophilic surface properties.[23]

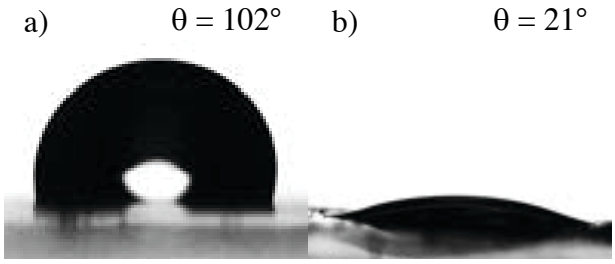

Figure 3: Sessile drop water contact angle on polystyrene a) before and b) after syngas treatment

When compared with the results obtained using ozone and previous results from other studies,[33, 36, 38, 58] this important drop in contact angle clearly demonstrates the effective surface modification of polystyrene through syngas PICVD under low energy UVC light. A sharp increase of the polar surface energy component (γ_s^p) was observed following the surface treatment, while the dispersive component (γ_s^d) only increased slightly. The total surface energy of polystyrene after treatment thus largely exceeds the normal range of 20-50 mJ/m^2 for most commercial commodity polymers (e.g. polyethylene, polypropylene and polystyrene).[54]

Table 1. Dynamic water contact angle measurements and surface energies for untreated and treated polystyrene surfaces

	Untreated PS	Treated PS	
		Syngas	Ozone
θ_{adv}^{w}(°)	101 ± 7	25 ± 6	26 ± 2
θ_{rec}^{w} (°)	78 ± 8	15 ± 2	22 ± 2
$\Delta\theta^{w}$ (°)	23 ± 15	10 ± 8	4 ± 4
θ_{adv}^{h} (°)	17 ± 5	10 ± 1	20 ± 5
γ_s (mJ/m^2)	31 ± 1	65 ± 2	70.1±0.4
γ_s^d (mJ/m^2)	26.6± 0.6	26.6±0.5	25.3±0.2
γ_s^p (mJ/m^2)	3.7 ± 0.8	38 ± 1	44.8±0.4

For untreated and treated samples, contact angle hysteresis is equal or higher than 4°, which indicates a level of surface non-ideality. Chemical homogeneity along the surface after treatment is inferred thanks to numerous contact angle measurements taken at different locations on the surface. Therefore, non-ideality can be caused either by surface roughness or by the coating interaction with the surrounding environment, if there is one. Surface roughness might arise when the coating grows according to an island growth mechanism. It occurs when the sum of surface energy of the coating (γ_s) and the interfacial energy (γ_i) is superior to the surface energy of the unmodified substrate (γ_s°). This can be assessed through the Bauer criterion $\Delta\gamma$:[62-63]

$$\Delta\gamma = \gamma_s + \gamma_i - \gamma_s^\circ \qquad (4)$$

When the Bauer criterion is superior to 0, an island growth mode occurs. On the contrary, a 2D layer-by-layer growth mode occurs when $\Delta\gamma < 0$. The interfacial energy (γ_i) is defined by Dupre's relation:

$$\gamma_i = \gamma_s^\circ + \gamma_s - \beta, \qquad (5)$$

where β corresponds to the adhesion energy. It is the work required to separate the coating from the substrate. The adhesion energy can be calculated from the dispersive and polar surface energy components of the treated (γ_s) and untreated (γ_s°) substrate according to the following equation:

$$\beta = 2\left(\sqrt{\gamma_s^d \gamma_s^{\circ d}} + \sqrt{\gamma_s^p \gamma_s^{\circ p}}\right) \qquad (6)$$

In our specific case, $\beta = 76.9$ mJ/m^2 and $\Delta\gamma = 53$ mJ/m^2. The underlying meaning of this highly positive value is that the coating process is likely through island growth. This hypothesis is further confirmed by the previous AFM results. If the coating indeed reacts with the environment and rearranges accordingly, one may suppose that the contact angle would not be maintained over time. Water contact angle measurements in air were performed over time on treated surfaces to verify the stability of the coating (Figure 4). A sharp increase in the contact angle occurs in the first 2 hours following the UV/ozone treatment and reaches a plateau at 59° one day after treatment, in line with other studies.[39, 42] Stability results for the syngas treatment show the same tendency as for ozone treatment, although the contact angle is systematically kept to a lower value of 35 ± 12° one day after treatment. Therefore, the hydrophobic recovery seems to be less pronounced after a syngas treatment than after a UV-ozone treatment.

The evolution in contact angle could be attributed to the desorption of loosely bonded oxygenated functional groups due to contact with water.[42] Loosely bonded groups could be a

consequence of ring scission and oxidation on the surface of polystyrene. Alternatively, since the system always wants to lower its free energy, the chemisorbed polymeric chains can quickly fold back on themselves when exposed to ambient air.[64] Oil contact angle measurements in water are needed to determine if this loss in hydrophilicity is due to one of these two mechanisms, or simply due to physical desorption, as it is the case with the UV-ozone treatment.

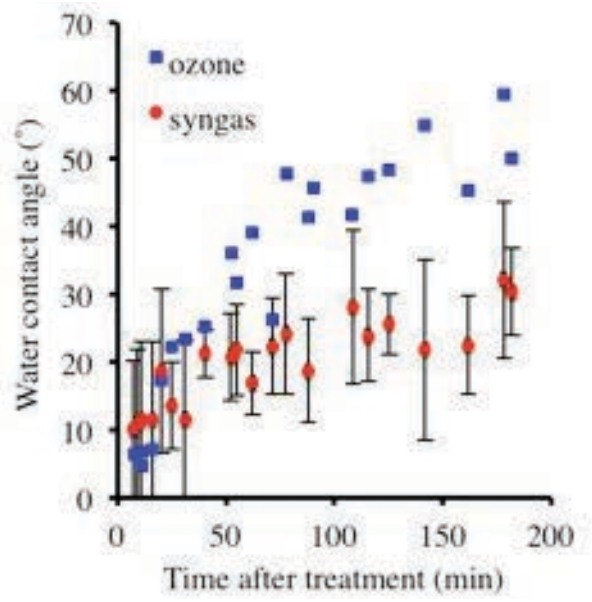

Figure 4: Stability of the ozone/UV functionalization over time

Silicon/Mineral Oils Contact Angle Measurements. In order to keep the free energy at the interface as low as possible, PICVD-treated polystyrene films were stored in DI water immediately after treatment. Since water is a polar medium, the oxygenated functional groups on the coating tend to stay on the surface. Mineral and organic oils of low viscosity were used to perform contact angle measurements in water (Figure 5).

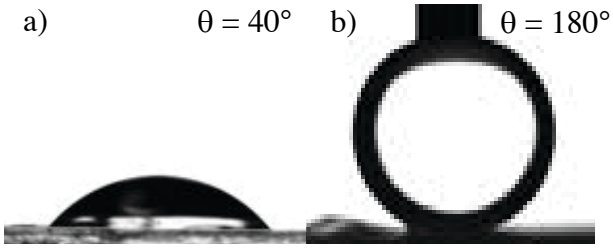

Figure 5: a) Silicone oil contact angle on polystyrene immersed in deionized water before treatment and b) after treatment

The drops were first dispensed both under and above untreated surfaces using an inverted and straight needle respectively. Contact angle measurements were similar in both cases, which means that the liquid density difference of silicon (mineral) oil with water does not significantly influence the measurements. Contact angle measurements for both untreated and treated samples are presented in tTable 2.

Table 2: Sessile drop contact angles of oils obtained on submerged samples (*180¡ means that the oil refused to wet the surface – would not detach from the goniometer syringe)

Oils	Untreated PS	Treated PS	
		Syngas	Ozone
Silicon	49 ± 9	165 ± 15	180 ± 0*
Mineral	27 ± 7	167 ± 13	174 ± 6

The treated PS films immersed in water were submitted to at least five oil contact angle measurements on different surface locations. In many cases, the oil drops were not even able to partially wet the treated surfaces. Videos of these results are provided as supporting information (S-2). Unlike the measurements conducted in air, the oil contact angles for samples stored in water remained stable more than one year after treatment. These results demonstrate the effective

and stable surface functionalization of polystyrene as long as the samples are stored in a polar media, which is their intended use in the production of stable challenge syringes. One interesting fact is that silicon oil is generally used to coat the inner walls of syringes, as a lubricant for the plunger. Given the treated PS surface s high contact angle with silicon oil, the treated PS-DVB beads aversion for the inner walls of validation syringes is already suspected.

FTIR spectroscopy. Both syngas and ozone treated polystyrene spectra exhibit a broad peak around 3400 cm^{-1}, which corresponds to the attachment of hydroxyl groups on the surface, and exhibit a sharper peak around 1720-1740 cm^{-1}, which is attributed to the presence of ketones, esters and carboxylic groups (

Figure **6**).

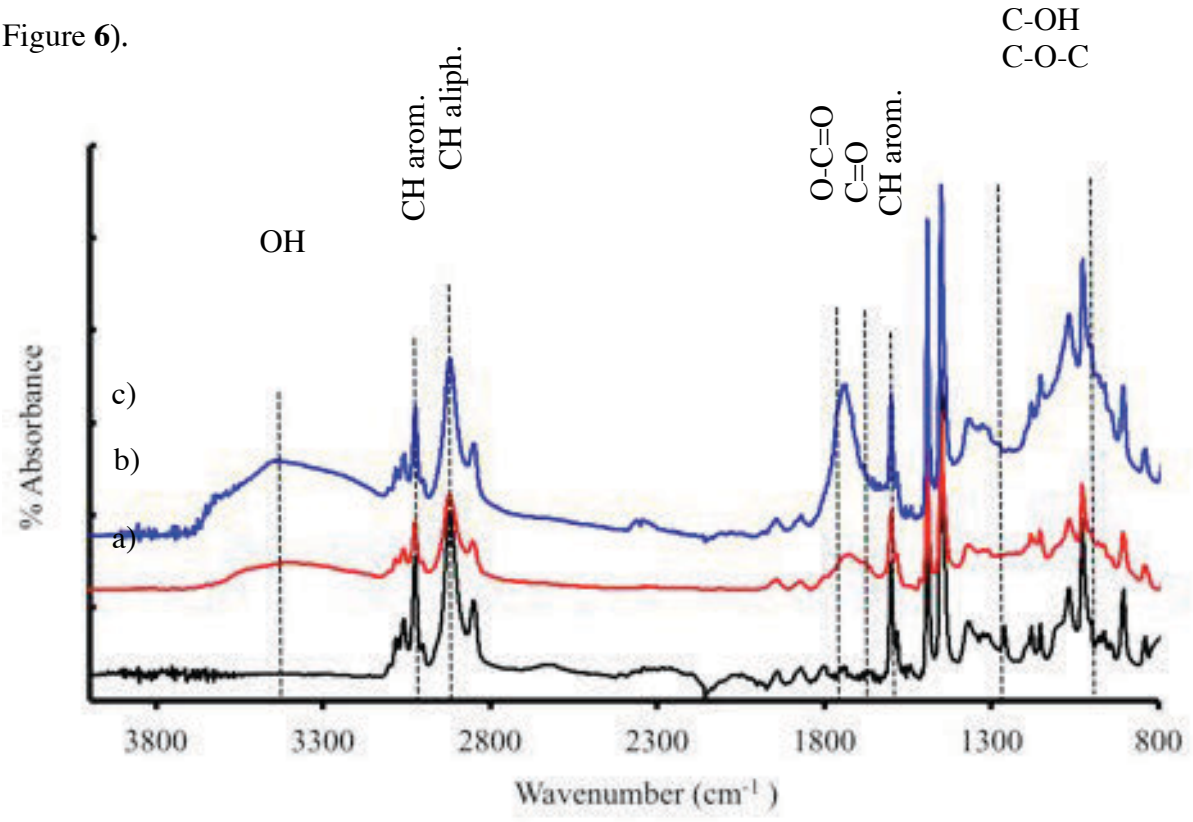

Figure 6: Infrared spectra of PS surfaces a) untreated, b) treated with syngas and c) treated with ozone

Moreover, an increase in the absorbance intensity compared with the untreated sample is observed around 1000-1300 cm^{-1} for both treatments, which corresponds to the presence of ether groups (C-O) in the surface. On the other hand, a decrease in the absorbance intensity for the π-bonds of the aromatic rings (1440-1490 cm^{-1}) as well as of the C-H aromatic and aliphatic bonds (2700-3300 cm^{-1}) compared to the untreated spectra is observed. For the ozone treated samples, the results are in good agreement with previous reports.[38-42, 59, 65] The syngas spectra are similar to those of polystyrene subjected to UVB light (300-400 nm) with an intensity of 45 mW/cm^2, in ambient air for one hour.[66] It is important to note however that the syngas spectra suffer from a lack of reproducibility, likely due to the low surface sensitivity of FTIR. Indeed, the surface analysis depth of 1-6.5 !m with FTIR might be greater than the coating thickness in the case of syngas treatment. The spectrum for syngas treatment illustrated in Figure 6 corresponds to our best FTIR result. On the other hand, the FTIR results for UV-ozone are perfectly reproducible, which could imply that the oxygenated species are housed in the deeper surface layers. A more sensitive surface characterization technique is required to confirm the efficiency of the syngas treatment.

X-Ray Photo-Electron Spectroscopy (XPS). With a maximum analysis depth of 10 nm, XPS is a much more surface sensitive technique to assess the presence of grafted functional groups on polystyrene. Survey spectra were first analyzed to assess the atomic content of the untreated and treated surfaces (Table 3). The polystyrene surface before treatment is mainly composed of carbon and a slight amount of oxygen due to silica contamination; this is often observed as silicon is a common additive to increase the flowability of polymeric raw materials.[37] The level of surface oxygen increased considerably after treatment with both precursors.

Table 3: Atomic species content of PS surfaces from survey spectra

	PS	PS treated	
	Untreated	Syngas	Ozone
C (%)	92 ± 5	43 ± 7	45 ± 2
O (%)	5 ± 3	46 ± 4	52.3±0.5
Si (%)	2 ± 2	4 ± 1	3 ± 1
Fe (%)	0	8 ± 5	0

Iron is also observed in the survey spectra of polystyrene treated with syngas. This iron might enter the PICVD reactor in the form of iron pentacarbonyl $Fe(CO)_5$, a compound often found in trace amounts (few ppm_v) inside pressurized carbon monoxide cylinders following extended storage.[67] High resolution analysis of the C1s peak (Figure 7) reveals the addition of C-O (286.6 eV), C=O (288 eV) and O=C-O (289 eV) functional groups on the surface after treatment for both syngas and ozone precursors. The presence of these new functional groups is further confirmed by the high-resolution analysis of O1s peak (Figure 8). After PICVD treatment, the carbon-carbon double bond (291.5 eV) from polystyrene s phenyl groups disappears completely due to oxidative cleavage (both precursors). The peaks at binding energies of 530.4 eV and 531.9 eV indicate oxygen bonding with a metal (Fe-O and FeOH respectively), likely from $Fe(CO)_5$. Indeed, this secondary compound can react with olefins through photochemical deposition when exposed to UV light. It first decomposes to iron tetracarbonyl and releases one CO group to react with a double bond and form an olefin-iron-tricarbonyl complex.[68] At first sight, it seems that the UV-ozone treatment adds more surface oxygen than the UV-syngas treatment.

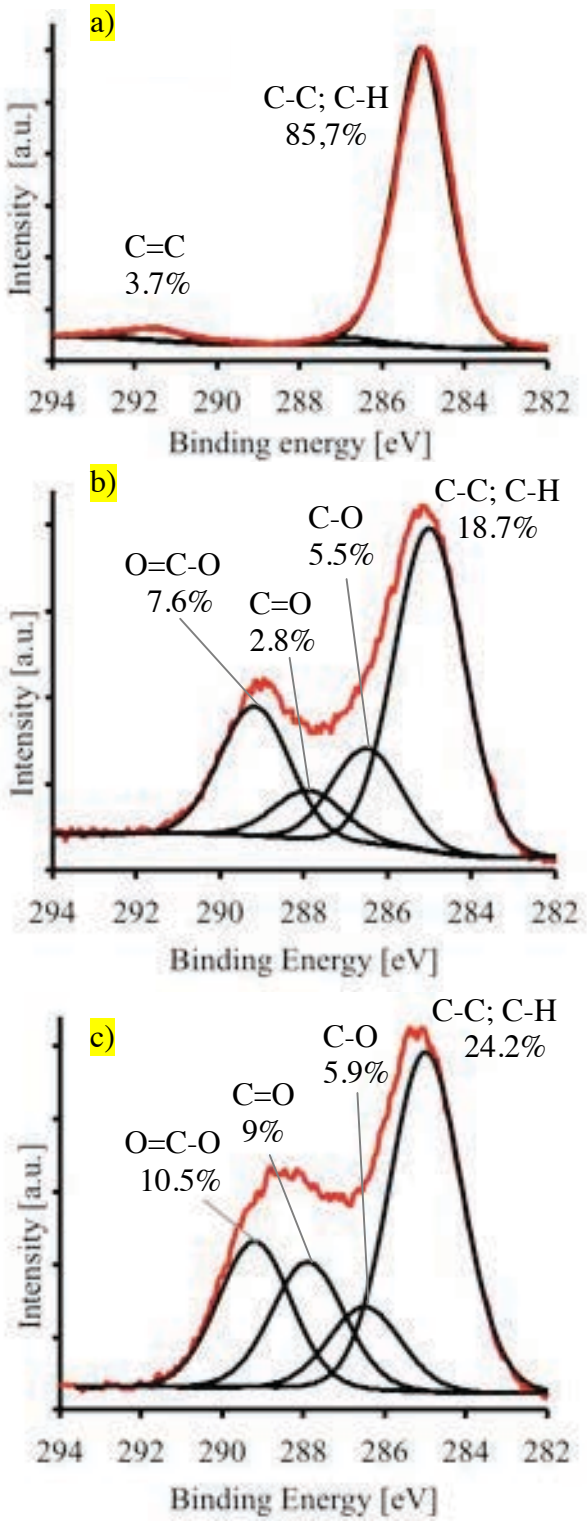

Figure 7: C1s XPS spectra of PS surfaces a) untreated, b) treated with syngas and c) treated

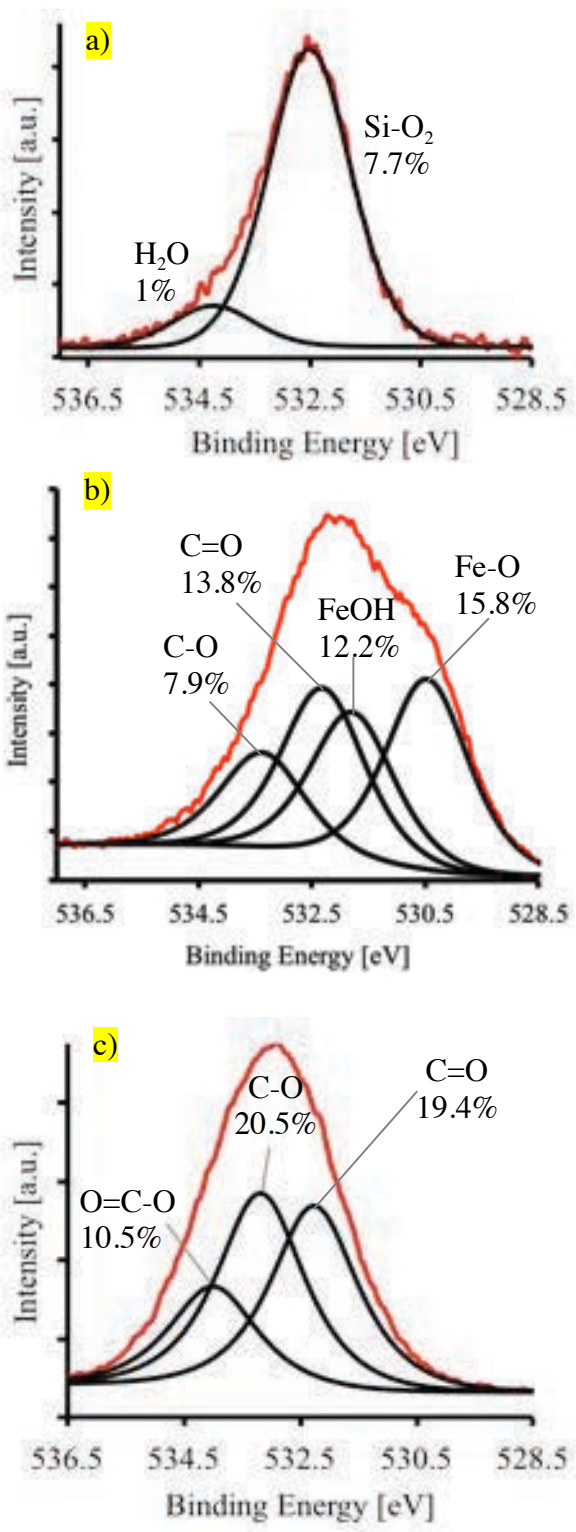

Figure 8: O1s XPS spectra of PS surfaces a) untreated, b) treated with syngas and c) treated with ozone

with ozone

However, when the percentages of oxygen bonding with carbon are compared in the C1s and O1s high resolution spectra for the UV-ozone treatment, it seems that the amount of carbon on the surface is not sufficient to bind all the oxygen atoms. The oxygen content reported in the survey spectra for the treatment with ozone exceeds by a factor of two the saturation content of 20-30% reported in the literature for UV-ozone treatments.[35, 42, 59] It is pertinent to note however that the samples discussed in the literature were subject to a water wash prior to analysis – we can therefore infer that approximately half of the oxygen atoms identified in the UV-ozone treatment are only physisorbed to the surface.

Zeta Potential Measurements. 5 !m-diameter PS-DVB beads were treated inside the reactor and subjected to zeta potential measurements immediately after treatment (Figure 9). PICVD functionalization with syngas decreases the zeta potential significantly. This increment in the zeta potential is higher than what has been reported for a polystyrene treatment with radio-frequency oxygen plasma.[27] By increasing the pH, the zeta potential of syngas-treated beads increases even more, which further confirms the presence of carboxylic groups on the surface. In principle, the presence of carboxylic groups favors the negative surface charge while the hydroxyl groups favors the positive surface charge.[69] On the other hand, almost no zeta potential increment was observed for ozone-treated beads. This lower increment might be attributable to the significant quantity of physisorbed oxygen species added to polystyrene, which would easily desorb from the surface. Indeed, previous studies reported that some of the ester, carboxylic and carbonyl groups that constitute the dominant surface groups after UV-ozone treatment of polystyrene can be removed by washing, while hydroxyl and ether remain on the surface.[34, 59] On

the other hand, most of the oxygen content on the surface would be covalently attached in the case of a UV-syngas treatment, which enables a better surface charge retention.

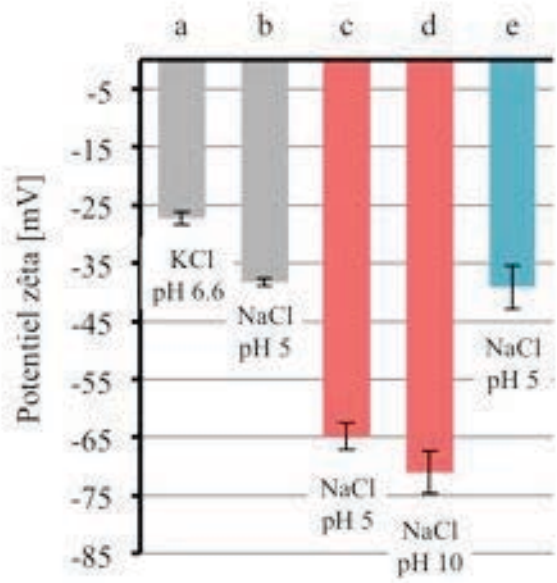

Figure 9. Zeta potential measurements of 5 μm PS-DVB beads a) untreated in 10 mM KCl, b) untreated in 10 mM NaCl, c) treated with syngas in 10 mM NaCl (pH 5), d) treated with syngas in 10 mM NaCl (pH 10) and e) treated with ozone in 10 mM NaCl

Proposed Reaction Mechanism. Using the compilation of all the previous results, a reaction mechanism between syngas, UV light and polystyrene can be proposed. The 254 nm UV light is an energy equivalent of 4.88 eV, sufficient for the cleavage of the π-bonds in polystyrene's phenyl groups[38, 43, 46, 70]. This provides reactive C-C* radical sites on the polystyrene surface from which a polymer-like cross-linked network can be synthesized. Carbon monoxide, dihydrogen and hydrogen peroxide also absorb the photon energy, thus creating the radicals *C=O, H*, O* and *OH in the gas phase. Numerous reactions are susceptible to occur inside the reactor: [48, 52]

1. $H_2O_2 + H^* \rightarrow H_2O + OH^*$

2.! $H_2O_2 + H^* \ \& \ {}^*O_2H + H_2$

3.! $H_2O_2 + OH^* \ \& \ H_2O + O_2^- + H^+$

4.! $C{\equiv}O + OH^* \ \& \ HO\text{-}C^+{=}O \ \& \ H^+ + CO_2$

5.! $H_2 + C{=}O^* \ \& \ C^+ + H_2O$

6.! $C{\equiv}O + C{=}O^* \ \& \ CO_2 + C^*$

7.! $C{\equiv}O + C^* \ \& \ C{=}O\text{-}C^*$

8.! $C_nO_{n-1} + CO \ \& \ C_{n+1}O_n$

9.! $C_{n+1}O_n + H_2 \ \& \ C_xH_yO_z + H_2O$

According to reactions 8 and 9, organic chain growth is susceptible to occur on the surface of polystyrene. The polystyrene photo-oxidation mechanism by UV-ozone is already extensively described in the literature[41, 70] and the results reported in this work are all consistent with what has already been observed in similar studies.

Dispersion Stability Testing. After characterization of polystyrene films and 5 !m beads, larger PS-DVB beads (100 !m, 200 !m and 500 !m) were treated inside the reactor using syngas as the precursor. The glass support was rotated 180 degrees halfway through the treatment to maximize the surface planes exposed to UV light and the gaseous precursors. The treated beads were then stored in water, until being seeded into validation syringes. The syringes were then vorticized at a speed of 3200 rpm for 2 seconds. Videos of the dispersion stability experiments are available as supporting information (S-3). Figure 10 compares the adhesion/dispersion behavior of both 200 μm untreated (a and b) and treated (c and d) PS-DVB beads, immediately after swirling.

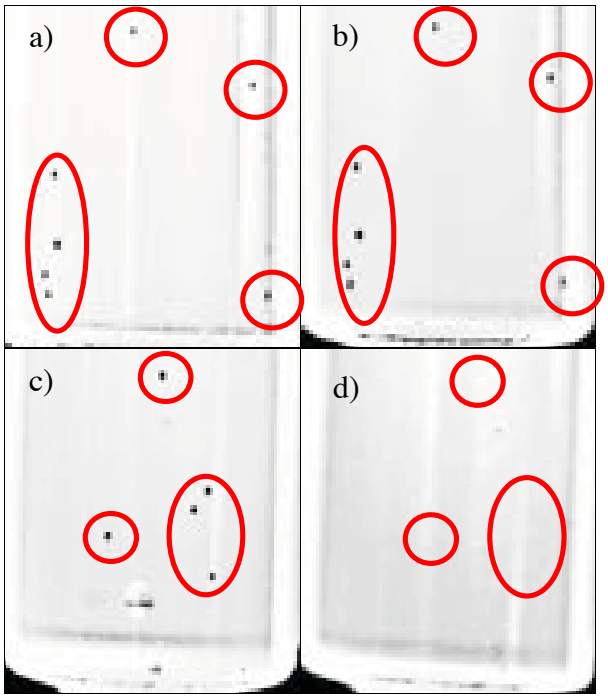

Figure 10. Untreated (a & b) and UV-syngas treated (c & d) 200 μm PS-DVB beads inside a washed syringe, before (a & c) and after (b & d) 2 seconds of vortex swirling

All treated beads were re-suspended following the swirling step, while the untreated beads remained adhered to the inner syringe walls. These observations hold true for each of the three beads sizes (100, 200 and 500 μm). These validation syringes were held at 58°C for two month to simulate ageing for two years. Each aged syringe was visually inspected to assess if the seeded bead either stays in suspension (suspension), peels off the inner walls following a swirling step at 3200 rpm for 2 seconds (reversible adhesion), or irreversibly sticks to the inner walls of the syringe (irreversible adhesion). This assessment was conducted after 1 month (1 year equivalent) and 2 months (2 year equivalent) (Figure 11). The UV-syngas surface treatment significantly improves the suspension behavior of the PS-DVB beads, and stability can be maintained for at least a two-year period for most bead sizes.

a)

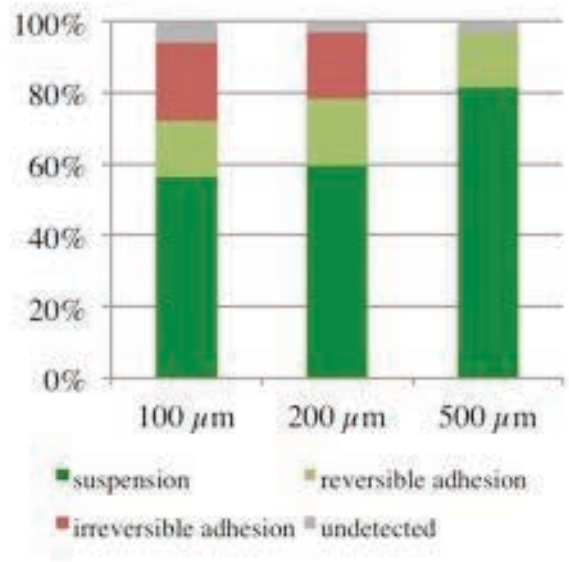

b)

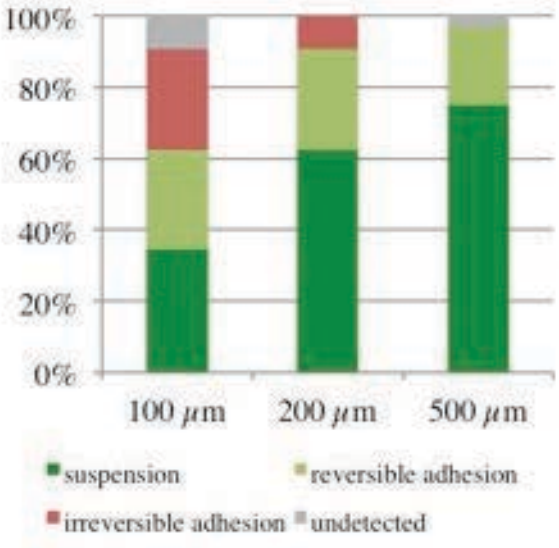

Figure 11: Percentages of a) one-year aged and b) two-year aged UV-syngas treated beads behavior in control syringes

Beads of 500 μm exhibits the best results, with 80% of the treated beads naturally in suspension inside the syringe and no irreversible adhesion reported. This could be explained by

their inherently larger surface, which causes them to be easily swept away by a vortex when compared to smaller beads. On the other hand, the 100 μm beads appear to be more affected by ageing: while over 70% exhibit at least partial stability after a one-year equivalency, this drops slightly to just over 60% after two years. In some cases, the seeded beads were not readily detected through visual inspection. In some cases, the bead became stuck inside the cap at the syringe tip (an issue often tackled in the pharmaceuticals industry).[8] Nevertheless, the fact remains that PICVD treatment using UVC as the energy source for activation and syngas as the precursor has proven effective in enhancing the dispersion behavior of PS-DVB beads.

CONCLUSION.

To prevent pulmonary emboli and other health issues, the pharmaceutical industry is managed by uncompromising quality control constraints, especially with regard to the detection of foreign particulates inside parenteral drugs. The low surface energy of standard beads seeded inside control syringes to mimic contamination hinders their detection because of irreversible adhesion to the syringes walls. A photo-induced chemical vapor deposition process using syngas as the precursor was used to modify the surface properties of PS-DVB standard beads in order to increase their surface energy and propensity to remain in suspension. Newly grafted C-OH, C-O-C, C=O and COOH functional groups were detected by XPS and FTIR characterization after treatment, leading to an increase in the surface energy from 31 ± 1 to 65 ± 2 mJ/m^2. Consequently, the zeta potential decreased from -38 mV to -61 mV after treatment. Finally, treated 100 μm, 200 μm and 500 μm PS-DVB beads suspended in water exhibited higher dispersion stability over time than untreated beads. These results show the potential of syngas PICVD to provide an effective solution to the issue of stability in challenge sets used in validation processes, thereby meeting the stringent quality control constraints imposed on

parenteral drugs, while making significant time and cost savings. This solution is also transposable to any other industry dealing with issues related to particle adhesion.

SUPPORTING INFORMATION

S: Supporting Information.

S-1: Detailed result of the experimental plan for surface treatment optimization (table) S-2: Contact angle measurements of silicone oil and mineral oil on untreated and treated polystyrene surfaces submerged in DI water (videos). S-3: Videos of stability dispersion testing of 200 μm PS-DVB beads inside a control syringe filled with Milli-Q water

AUTHOR INFORMATION

Corresponding Author

*E-mail: jason.tavares@polymtl.ca

Tel. : +1 (514) 340-4711 ext 2326

Author Contributions

The manuscript was written through contributions of all authors. All authors have given approval to the final version of the manuscript.

Notes The authors declare no competing financial interest.

ACKNOWLEDGMENTS

This work was financially supported by the Natural Sciences and Engineering Research Council of Canada (CRD, RTI Category 1), the Canadian Foundation for Innovation and Liebel-Flarsheim Canada Inc. Pharmaceuticals. This work has benefited from collaboration with Nathalie Tufenkji (Biocolloids and Surface Laboratory, McGill University), Pierre M. Tremblay and Patricia Moraille (Materials Characterization Laboratory, Université de Montréal), and Josianne Lefebvre (Laboratory for the Analysis of the Surface of Materials - LASM, Polytechnique Montreal).

ABBREVIATIONS

PICVD, Photo-Induced Chemical Vapor Deposition

PS, Polystyrene

PS-DVB, Polystyrene-Divinyl-Benzene

WFI, Water for Injection

DI, Deionized

CAM, Contact Angle Measurements

γ_w^d, dispersive component of water surface tension

γ_w^p, polar component of water surface tension

γ_h^d, dispersive component of n-hexadecane surface tension

γ_h^p, polar component of n-hexadecane surface tension

γ_{PS}, polystyrene surface energy

γ_{PS}^{d}, dispersive component of polystyrene surface energy

γ_{PS}^{p}, polar component of polystyrene surface energy

θ_{adv}^{w}, advancing contact angle of deionized water

θ_{adv}^{h}, advancing contact angle of n-hexadecane

θ_{rec}^{w}, receeding contact angle of deionized water

REFERENCES

(1) *Pre-filled Syringes Market, 2013-2023*; Product Code RA10003; Roots Analysis Private Ltd.: 1 July 2013, p 156.

(2) Langille S. E., Particulate Matter in Injectable Drug Products. *PDA J Pharm Sci Technol.* **2013,** *67* (3), 186-200.

(3) Reedy J. S.; Kuhlman J. E.; Voytovich M., Microvascular Pulmonary Emboli secondary to Precipitated Crystals in a Patient receiving Total Parenteral Nutrition*: A Case Report and Description of the High-Resolution ct Findings. *Chest* **1999,** *115* (3), 892-895.

(4) Arnett E. N.; Battle W. E.; Russo J. V.; Roberts W. C., Intravenous Injection of Talc-Containing Drugs intended for Oral Use: a Cause of Pulmonary Granulomatosis and Pulmonary Hypertension. *Am. J. Med.* **1976,** *60* (5), 711-718.

(5) Hill S. E.; Heldman L. S.; Goo E. D.; Whippo P. E.; Perkinson J. C., Fatal Microvascular Pulmonary Emboli from Precipitation of a Total Nutrient Admixture Solution. *J Parenter Enteral Nutr* **1996,** *20* (1), 81-87.

(6) Brown K. T., Fatal Pulmonary Complications after Arterial Embolization with 40–120-m Tris-Acryl Gelatin Microspheres. *J Vasc Interv Radiol* **2004,** *15* (2), 197-200.

(7) Rathore N.; Chen C.; Gonzalez O.; Ji W. Challenges and Strategies for Implementing Automated Visual Inspection for Biopharmaceuticals. *Pharmaceutical Technology* [Online], 2009. http://www.pharmtech.com/challenges-and-strategies-implementing-automated-visual-inspection-biopharmaceuticals (accessed Jan 20, 2016).

(8) Melchore J. A.; Berdovich D., Considerations for Design and Use of Container Challenge Sets for Qualification and Validation of Visible Particulate Inspection. *PDA J Pharm Sci Technol.* **2012,** *66* (3), 273-284.

(9) Shabushnig J. G., Hot Topics in the Visual Inspection of Injectable Products. Pfizer Global Quality Operations ed.; 2011.

(10) Forcino H. Trends and best Practices in Visual Inspection. *Pharm. Technol.* [Online], 2014. http://www.pharmtech.com/trends-and-best-practices-visual-inspection (accessed Jan 01, 2016).

(11) Spak D., Baxter Voluntarily Initiates U.S. Recall of Two Lots of Peritoneal Dialysis Solution Due to Presence of Particulate Matter. Food and Drug Administration: United States, 2014.

(12) Bradley D., Cephalon Inc. issues a Voluntary Nationwide Recall of Treanda (bendamustine HCL) for Injection 25mg/Vial Due to Particulate Matter. Food and Drug Administration: 2012.

(13) HOSPIRA, Hospira Issues Voluntary Nationwide Recall of Three Lots of Carboplatin Injection Due to Visible Particulate Matter. Food and Drug Administration: 2014.

(14) Shnek D.; Carion-Martinez M.; Gigh A.; Segarra E.; Bruno M.; Aquino A.; Paranandi M., Comparing Manual and Automated Inspection of Seeded Syringe Defects. In *PDA Visual Inspection Forum*, Bethesda, 2007.

(15) Deng S.; Shnek D.; Carrion-Martinez M.; Dompenciel R.; Baez L.; Sullivan J.; Sing, N.; Ruhl, S., Evaluation of Automated Visual Inspection (AVI) Technologies for Biologic Products. In *PD Annual Meeting*, Las Vegas, 2009.

(16) Wang Z.; Huang Y.; Li S.; Xu H.; Linder M. B.; Qiao M., Hydrophilic modification of polystyrene with hydrophobin for time-resolved immunofluorometric assay. *Biosensors & bioelectronics* **2010,** *26* (3), 1074-9.

(17) Murakami T. N.; Fukushima Y.; Hirano Y.; Tokuoka Y.; Takahashi M.; Kawashima N., Surface modification of polystyrene and poly(methyl methacrylate) by active oxygen treatment. *Colloids and Surfaces B: Biointerfaces* **2003,** *29* (2–3), 171-179.

(18) Lee W.-F.; Lee H.-H., Surface Graft Modification of Styrene Butadiene Styrene Triblock Copolymer Membrane by Ultraviolet Irradiation. *Journal of Elastomers and Plastics* **2010,** *42* (1), 49-64.

(19) Fugaru V.; Bubueanu G.; Tuta C., Radiation induced grafting of acrylic acid onto extruded polystyrene surface. *Radiation Physics and Chemistry* **2012,** *81* (9), 1345-1348.

(20) Mielczarski J.; Jeyachandran Y.; Mielczarski E.; Rai B., Modification of polystyrene surface in aqueous solutions. *Journal of colloid and interface science* **2011,** *362* (2), 532-539.

(21) Wang L.; Yan L.; Zhao P.; Torimoto Y.; Sadakata M.; Li Q., Surface Modification of Polystyrene with Atomic Oxygen Radical Anions-Dissolved Solution. *Appl. Surf. Sci.* **2008,** *254* (13), 4191-4200.

(22) Dorval Dion C. A.; Tavares J. R., Photo-initiated chemical vapor deposition as a scalable particle functionalization technology (a practical review). *Powder Technology* **2013,** *239,* 484-491.

(23) Sasai Y.; Komatsu A.; Kondo S.; Yamauchi Y.; Kuzuya M., Fabrication of Hydrophilic Polymer Brushes on Polystyrene Substrate by Plasma-based Surface Functionalization. *Journal of Photopolymer Science and Technology* **2012,** *25* (4), 551-554.

(24) YOSHIHISA K.; YOSHIMURA A.; SHIBAMORI Y.; FUCHIGAMI K.; KUBOTA N., Hydrophilic Modification of Plastic Surface by using Microwave Plasma Irradiation. *IHI Engineering Review* **2013,** *46* (1), 5.

(25) Guruvenket S.; Rao G. M.; Komath M.; Raichur A. M., Plasma surface modification of polystyrene and polyethylene. *Applied Surface Science* **2004,** *236* (1–4), 278-284.

(26) Callen B.; Ridge M.; Lahooti S.; Neumann A.; Sodhi R., Remote Plasma and Ultraviolet–Ozone Modification of Polystyrene. *Journal of Vacuum Science & Technology A* **1995,** *13* (4), 2023-2029.

(27) Dupont-Gillain C. C.; Adriaensen Y.; Derclaye S.; Rouxhet P., Plasma-oxidized polystyrene: wetting properties and surface reconstruction. *Langmuir : the ACS journal of surfaces and colloids* **2000,** *16* (21), 8194-8200.

(28) Vegh J.; Nest D.; Graves D.; Bruce R.; Engelmann S.; Kwon T.; Phaneuf R.; Oehrlein G.; Long B.; Willson C., Near-surface modification of polystyrene by Ar+: Molecular dynamics simulations and experimental validation. *Applied Physics Letters* **2007,** *91* (23), 233113.

(29) Ionita M.; Da'an B.; Teodorescu M.; Mutlu M.; Mitu B.; Dinescu G., Surface modification of polystyrene beads using RF atmospheric pressure plasma jet.

(30) Kong J.; Yung K.; Xu Y.; Tian W., Wettability transition of plasma-treated polystyrene micro/nano pillars-aligned patterns. *Express Polym. Lett* **2010,** *4* (12), 753-762.

(31) Kuo Y.-L.; Chang K.-H.; Hung T.-S.; Chen K.-S.; Inagaki N., Atmospheric-pressure plasma treatment on polystyrene for the photo-induced grafting polymerization of N-isopropylacrylamide. *Thin Solid Films* **2010,** *518* (24), 7568-7573.

(32) Bagheri-khoulenjani S.; Mirzadeh H., Polystyrene surface modification using excimer laser and radio-frequency plasma: blood compatibility evaluations. *Prog Biomater* **2012,** *1* (1), 1-8.

(33) Pfleging W.; Torge M.; Bruns M.; Trouillet V.; Welle A.; Wilson S., Laser-and UV-assisted modification of polystyrene surfaces for control of protein adsorption and cell adhesion. *Applied Surface Science* **2009,** *255* (10), 5453-5457.

(34) Browne M.; Lubarsky G.; Davidson M.; Bradley R., Protein Adsorption onto Polystyrene Surfaces studied by XPS and AFM. *Surf. Sci.* **2004,** *553* (1), 155-167.

(35) Muntean S. A.; Kemper M.; van IJzendoorn L. J.; Lyulin A. V., Roughness and Ordering at the Interface of Oxidized Polystyrene and Water. *Langmuir.* **2011,** *27* (14), 8678-8686.

(36) Huang W.; Fan H.; Zhuang X.; Yu J., Effect of UV/Ozone Treatment on Polystyrene Dielectric and its Application on Organic Field-Effect Transistors. *Nanoscale Res Lett* **2014,** *9* (1), 1-8.

(37) Lubarsky G.; Davidson M.; Bradley R., Characterisation of Polystyrene Microspheres Surface-Modified using a Novel UV-Ozone/Fluidised-Bed Reactor. *Appl. Surf. Sci.* **2004,** *227* (1), 268-274.

(38) Yusilawati A. N.; Maizirwan M.; Hamza M. S.; Ng K. G.; Wong C. S., Surface Modification of Polystyrene beads by Ultraviolet/ozone Treatment and its effect on gelatin coating. *American Journal of Applied Sciences* **2010,** *7* (6), 724-731.

(39) Roth A. D. CHEMICAL MODIFICATION OF POLYSTYRENE AND GOLD SURFACES. Cornell University, United States, 2009.

(40) Murakami T. N.; Fukushima Y.; Hirano Y.; Tokuoka Y.; Takahashi M.; Kawashima N., Surface modification of polystyrene and poly (methyl methacrylate) by active oxygen treatment. *Colloids and Surfaces B: Biointerfaces* **2003,** *29* (2), 171-179.

(41) Murakami T. N.; Fukushima Y.; Hirano Y.; Tokuoka Y.; Takahashi M.; Kawashima N., Modification of PS films by combined treatment of ozone aeration and UV irradiation in aqueous ammonia solution for the introduction of amine and amide groups on their surface. *Applied surface science* **2005,** *249* (1), 425-432.

(42) Davidson M.; Mitchell S.; Bradley R., Surface studies of low molecular weight photolysis products from UV-ozone oxidised polystyrene. *Surface science* **2005,** *581* (2), 169-177.

(43) Hozumi A.; Inagaki H.; Kameyama T., The hydrophilization of polystyrene substrates by 172-nm vacuum ultraviolet light. *Journal of colloid and interface science* **2004,** *278* (2), 383-392.

(44) Kirschner M. J., Ozone. In *Ullmann's Encyclopedia of Industrial Chemistry*, Wiley-VCH Verlag GmbH & Co. KGaA: 2000.

(45) Tr panier M.; Dion C. A. D.; Dalai A. K.; Abatzoglou N., Kinetics Study on Cnt¦Supported RuKCo FTS Catalyst in a Fixed Bed Reactor. *Can. J. Chem. Eng.* **2011,** *89* (6), 1441-1450.

(46) Arvidsson A.; White J., Densification of Polystyrene under Ultraviolet Irradiation. *J. Mater. Sci. Lett.* **2001,** *20* (23), 2089-2090.

(47) Elimelech M.; Gregory J.; Jia X.; Williams R. A.; Gregory J.; Jia X.; Williams R. A., Chapter 3 - Surface interaction potentials. In *Particle Deposition & Aggregation*, Elimelech, M.; Gregory, J.; Jia, X.; Williams, R. A.; Williams, J. G. J. A., Eds. Butterworth-Heinemann: Woburn, 1995; pp 33-67.

(48) Dorval Dion C. A.; Raphael W.; Tong E.; Tavares J. R., Photo-initiated chemical vapor deposition of thin films using syngas for the functionalization of surfaces at room temperature and near-atmospheric pressure. *Surface and Coatings Technology* **2014,** *244*, 98-108.

(49) Dion C. A. D. D position photochimique du gaz de synth se (CO et H2) pour la fonctionnalisation en surface conditions ambiantes. cole Polytechnique de Montr al, Montreal, 2013.

(50) Javanbakht T.; Raphael W.; Tavares J. R., Physicochemical Properties of Nanocrystalline Cellulose Treated by Photo-Initiated Chemical Vapor Deposition (PICVD). *Can J Chem Eng* **2015**, 17 pp.

(51) Javanbakht T.; Laurent S.; Stanicki D.; Raphael W.; Tavares J. R., Charge effect of superparamagnetic iron oxide nanoparticles on their surface functionalization by photo-initiated chemical vapour deposition. *J Nanopart Res* **2015,** *17* (12), 462.

(52) Farhanian D.; Dorval Dion C. A.; Raphael W.; De Crescenzo G.; Tavares J. R., Combined Extraction and Functionalization of low-cost Nanoparticles from Municipal Solid Waste Fly Ash through PICVD. *J. Env. Chem. Eng.* **2014,** *2* (4), 2242-2251.

(53) Dalet P.; Papon E.; Villenave J. J., Surface free energy of polymeric materials : relevancy of conventional contact angle data analyses. *Journal of Adhesion Science and Technology* **1999,** *13* (8), 857-870.

(54) DataPhysics, Surface Tension Values of some common Test Liquids for Surface Energy Analysis. Nov 24, 2006 ed.

(55) (enkiewicz M., Comparative study on the surface free energy of a solid calculated by different methods. *Polymer Testing* **2007,** *26* (1), 14-19.

(56) VandeVen T., Electrokinetics of Colloids. In *CHEM 585- Colloid Chemistry*, McGill: Montreal, 2015.

(57) ASTM, Standard Guide for Accelerated Aging of Sterile Barrier Systems for Medical Devices. ASTM: Pennsylvania, 2011; Vol. F1980-07, p 7.

(58) Hemmerich K. J., General Aging Theory and Simplified Protocol for Accelerated Aging of Medical Devices. *Med. Plast. Biomat.* **1998**, 16-23.

(59) Teare D.; Ton!That C.; Bradley R., Surface characterization and ageing of ultraviolet–ozone!treated polymers using atomic force microscopy and x!ray photoelectron spectroscopy. *Surface and interface analysis* **2000,** *29* (4), 276-283.

(60) Callen B.; Ridge M.; Lahooti S.; Neumann A.; Sodhi R., Remote Plasma and Ultraviolet–Ozone Modification of Polystyrene. *J. Vac. Sci. Technol., A* **1995,** *13* (4), 2023-2029.

(61) Ge D.; Li Y.; Yang L.; Fan Z.; Liu C.; Zhang X., Improved self-assembly through UV/ozone surface-modification of colloidal spheres. *Thin Solid Films* **2011,** *519* (15), 5203-5207.

(62) Niyamakom P. Influence of Deposition Parameters on Morphology, Growth and Structure of Crystalline and Amorphous Organic Thin Films (the case of Perylene and alpha-NPD). PhD Dissertation, RWTH Aachen University, June 20, 2008.

(63) Wuttig M.; Liu X., *Ultrathin metal films: magnetic and structural properties*. Springer Science & Business Media: 2004; Vol. 206, p 376

(64) Occhiello E.; Morra M.; Cinquina P.; Garbassi F., Hydrophobic Recovery of Oxygen-Plasma-treated Polystyrene. *Polymer* **1992,** *33* (14), 3007-3015.

(65) Romero-S nchez M. D.; Pastor-Blas M. M.; Mart n-Mart nez J. M.; Walzak M., Addition of ozone in the UV radiation treatment of a synthetic styrene-butadiene-styrene (SBS) rubber. *International journal of adhesion and adhesives* **2005,** *25* (4), 358-370.

(66) Kanda-Nishikicho; Chiyoda-ku. Deterioration of UV-Irradiation Resin by FTIR and DUH-211S Dynamic Ultra Micro Hardness Tester by Shimadzu. *Shimadzu Application News* [Online], 2012. http://www.azom.com/article.aspx?ArticleID=7676 (accessed Oct 26, 2012).

(67) Williams T. C.; Shaddix C. R., Contamination of Carbon Monoxide with Metal Carbonyls: Implications for Combustion Research. *Combust. Sci. Technol.* **2007,** *179* (6), 1225-1230.

(68) Flenniken C. L. Phase Separation of Metal or Metal-Oxide Microparticles in Solid Polymer Matrices. PhD dissertation, University of Florida, USA, 1984.

(69) Malvern. Zeta Potential - An introduction in 30 minutes *Zetasizer Nano series technical note* [Online]. http://www3.nd.edu/~rroeder/ame60647/slides/zeta.pdf (accessed Feb 5, 2016).

(70) Klein R. J.; Fischer D. A.; Lenhart J. L., Systematic Oxidation of Polystyrene by Ultraviolet-Ozone, characterized by Near-Edge X-Ray Absorption Fine Structure and Contact Angle. *Langmuir.* **2008,** *24* (15), 8187-8197.

Synopsis

Container challenge sets, used in the qualification and validation of automated visible particle inspection systems, are prepared by seeding a single standardized polystyrene-divinylbenzene (PS-DVB) bead inside the commercial product to mimic foreign particulates. Due to its low surface energy and wettability, the bead adheres to container walls, hindering its detection by the motion based inspection system. The aim of this research is to modify the surface properties of the bead in such a way that it repulses the inner walls and stays in suspension inside the liquid product. The surface treatment consists of a photo-induced chemical vapor deposition (PICVD) process using syngas and UVC light. Following treatment, newly grafted C-OH, C-O-C, C=O and COOH functional groups on the bead's surface are observed by XPS and FTIR spectroscopy, leading to an increase in the surface energy from 31 ± 1 to 65 ± 2 mJ/m^2, and a corresponding zeta potential decrease from -38 mV to -61 mV. Finally, treated 100 μm, 200 μm and 500 μm PS-DVB beads suspended in water exhibit higher dispersion stability over time than untreated beads. These results show the potential of syngas PICVD to provide an effective solution to the stability issue of containers challenge sets for the validation of automated particle inspection systems, enabling significant savings of time and money to the parenteral drug industry.

Table of Contents (TOC) Graphic